Eur. Phys. J. D (2016) 70: 162
DOI: 10.1140/epjd/e2016-60638-3

THE EUROPEAN PHYSICAL JOURNAL D

Regular Article

Fast controlled preparation of two-atom maximally entangled state and N-atom W state in the direct coupled cavity systems via shortcuts to adiabatic passage

Zhe Wang[1], Yan Xia[1,a], Ye-Hong Chen[1], and Jie Song[2]

[1] Department of Physics, Fuzhou University, Fuzhou 350002, P.R. China
[2] Department of Physics, Harbin Institute of Technology, Harbin 150001, P.R. China

Received 10 November 2015 / Received in final form 18 March 2016
Published online 30 August 2016 –

Abstract. We propose a scheme to fast controlled preparation of two-atom maximally entangled state and N-atom W state in the directly coupled cavities systems via shortcuts to adiabatic passage (STAP). Numerical simulation demonstrates that the scheme is faster than adiabatic passage and robust against the decoherence caused by atomic spontaneous emission and photon leakage. The result provides a theoretical basis for the manipulation of quantum states in the directly coupled cavities systems via STAP and contributes to the understanding of more complex systems.

1 Introduction

Quantum entanglement, one of the most intriguing properties in quantum mechanics, is a key resource for quantum information processing (QIP) [1,2], such as quantum teleportation [3], quantum dense coding [4], quantum cryptography [5], quantum computation [6], and so on. Typical entangled states are the Bell states [7], the Greenberger-Horne-Zeilinger (GHZ) states [8,9], and the W states [10]. Different entangled states have different advantages. For instance, the Bell states are the two-particle entangled states which are fundamental for demonstrating quantum nonlocality [7]. The GHZ states provide possibilities for testing quantum mechanics against local hidden variable theory [11]. Compared with the above two types of entangled states, the W states possess a high degree of robustness against the qubit loss as they maintain some entanglement when more than two qubits remains. Many entangled states' preparation programs have been realized in ion traps [12], cavity quantum electrodynamics (QED) systems [13,14], and other systems. Among these systems, coupled cavities QED systems have the advantages of easily addressing individual lattice sites with external control and scalability, which give the possibility to compose a quantum network. Thus, much attention has been paid to the investigation of coupled cavities systems [15–18] in recent years.

There are two major routes for generating and manipulating the entangled states with external interacting fields. One is fixed-area resonant pulses route [19–21] and the other is the adiabatic method [22–24]. In general terms, simple fixed-area resonant pulses may be fast if intense enough, but the schemes are difficult to implement since all parameters need to be precisely controlled. That is, the fidelity is highly sensitive to the parameters fluctuations. The advantage of the adiabatic method is that it can reduce populations of the intermediate excited states. Therefore, the method would restrain the influence of atomic spontaneous emission on the fidelity. However, in order to make sure each of the eigenstates of the system evolves along itself all the time without transition to other ones, the controlling parameters should change slowly enough. Thus, the adiabatic method typically needs long evolution time [25]. However, it should be avoided, because decoherence, noise, or losses would spoil the intended dynamics. Therefore, a fast, robust and easy to realize scheme is important to generate and manipulate entangled states.

To achieve fast and high-fidelity quantum states, some approaches [26–45] have been proposed. For example, Masuda and Nakamura [27] have proposed the theory of the fast-forward of adiabatic dynamics in quantum mechanics. The theory can accelerate quantum dynamics by using an additional phase of a wave function and obtain a target state in any desired short time. Berry [33] has put forward "Transitionless quantum driving" (TQD) to construct the "counter-diabatic driving" (CDD) Hamiltonian $H(t)$, which can accurately derive the instantaneous eigenstates of $H_0(t)$ to effectively speed up adiabatic processes. Chen et al. [34] have present a reverse-engineering approach which use the Lewis-Riesenfeld (LR) invariant to carry the eigenstates of a Hamiltonian from a specified initial to a final configuration, and then design the transient Hamiltonian from the LR invariant. Soon afterwards, Chen and Muga [36] have proposed a scheme to perform a fast population transfer (FPT) in three-level

[a] e-mail: xia-208@163.com

systems under the help of the inverse engineering based on LR invariant. Palmero et al. [37] have designed fast trajectories of a trap to transport two ions using shortcut-to-adiabaticity technique based on invariants. Inspired by these works and in combination with quantum Zeno dynamics (QZD) [46,47], Chen et al. [44] have constructed shortcuts for performing the FPT of ground states in multiparticle systems with invariant-based reverse engineering in cavity QED systems. We note that references [42–45] have successfully introduced shortcuts to adiabatic passage (STAP) into cavity QED systems, but, so far, fast controlled preparation of multiparticle entangled states in the directly coupled cavities systems has not been put forward because it is hard to directly generalize the idea in references [42–45]. In view of that we ask if it is possible to construct STAP for multiparticle in the directly coupled cavities systems.

In our scheme, we use the inverse engineering based on LR invariant to construct effective STAP for speeding up the generation rate of the two-atom maximally entangled state and N-atom W state in the directly coupled cavities systems. Compared with previous works, the present scheme has the following advantages. First, we realize the fast controlled preparation of two-atom maximally entangled state and N-atom W state in the $N+1$ directly coupled cavities via STAP. That is, we take one of the $N+1$ atoms as the control qubit and the rest of N atoms as the controlled qubits. Secondly, the $N+1$ atoms are trapped in the $N+1$ cavities, respectively. So, our scheme avoids the influence of direct interaction among atoms and also makes the individual addressing easy. Furthermore, due to the spatial separation of each qubit, it is feasible to control every single qubit by laser pulse in experiment. Thirdly, numerical simulation shows that our scheme has a high fidelity and the evolution process is fast. Besides, our scheme is robust against parameters fluctuation in the experimental and decoherence caused by atomic spontaneous emission and photon leakage. Fourthly, we propose a scheme to generate entangled state in the $N+1$ directly coupled cavities, this work maybe helpful for large-scale quantum information processing.

This paper is organized as follows. In Section 2, we show that the fast controlled preparation of two-atom maximally entangled state can be realized in the three directly coupled cavities via STAP. In Section 3, we use STAP to realize the fast controlled preparation of N-atom W state in the $N+1$ directly coupled cavities. In Section 4, we provide the numerical simulation and discussion. The conclusion is in Section 5.

2 Fast controlled preparation of two-atom maximally entangled state in 3 directly coupled cavities via Shortcuts to adiabatic passage

We consider that three Λ-type atoms 1, 2, and 3 are trapped in three directly coupled cavities c_1, c_2, and c_3,

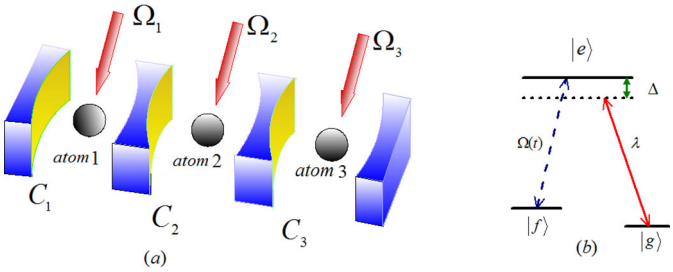

Fig. 1. (a) The cavity-atom combined system for controlled two-atom maximally entangled state generation. (b) The atomic level configuration.

respectively (here, we choose the second atom as the control qubit). The involved atomic levels and transitions are depicted in Figure 1, each atom has an excited state $|e\rangle$ and two ground states $|f\rangle$ and $|g\rangle$. The atomic transition $|f\rangle_k \leftrightarrow |e\rangle_k$ $(k = 1, 2, 3)$, where subscript k denotes the kth atom, is resonantly driven through a time-dependent laser pulse with Rabi frequency $\Omega_k(t)$, and the transition $|g\rangle_k \leftrightarrow |e\rangle_k$ is non-resonantly coupled to the cavity mode with coupling constant λ_k and detuning Δ. The whole Hamiltonian in the interaction picture is written as $(\hbar = 1)$

$$
\begin{aligned}
H_i &= H_{al} + H_{ac} + H_c, \\
H_{al} &= \sum_{k=1,2,3} \Omega_k(t)|e\rangle_k\langle f| + H.c., \\
H_{ac} &= \sum_{k=1,2,3} \lambda_k a_k e^{i\Delta t}|e\rangle_k\langle g| + H.c., \\
H_c &= \sum_{n=1,2} v a_n^\dagger a_{n+1} + H.c.,
\end{aligned} \tag{1}
$$

where $a_n^\dagger$ and a_n (subscript n denotes cavity number) are the creation and annihilation operators for photons, respectively. v denotes the hopping rate between the adjacent cavities. For convenience, we assume $\Omega_k(t)$, λ_k, and v to be real. Next, we rewrite the Hamiltonian in terms of new bosonic operators $q_1 = \frac{1}{\sqrt{2}}(a_3 - a_1)$, $q_2 = \frac{1}{2}(a_1 + \sqrt{2}a_2 + a_3)$, and $q_3 = \frac{1}{2}(a_1 - \sqrt{2}a_2 + a_3)$. Then, the Hamiltonian in the interaction picture can be written as:

$$
\begin{aligned}
H_i &= H_{al}^I + H_{ac}^I + H_c^I, \\
H_{al}^I &= \sum_{k=1,2,3} \Omega_k(t)\,|e\rangle_k\langle f| + H.c., \\
H_{ac}^I &= \lambda_1|e\rangle_1\langle g|\frac{1}{2}\left(-\sqrt{2}q_1 + q_2 + q_3\right)e^{i\Delta t} \\
&\quad + \lambda_2|e\rangle_2\langle g|\frac{1}{\sqrt{2}}\left(q_2 - q_3\right)e^{i\Delta t} \\
&\quad + \lambda_3|e\rangle_3\langle g|\frac{1}{2}\left(\sqrt{2}q_1 + q_2 + q_3\right)e^{i\Delta t} + H.c., \\
H_c^I &= \sqrt{2}v\left(q_2^\dagger q_2 - q_3^\dagger q_3\right).
\end{aligned} \tag{2}
$$

In the rotation framework, we perform the unitary transformation $U = e^{iH_c^I t}$. After that, we obtain the effective Hamiltonian H_I

$$\begin{aligned}
H_I &= H_{al}^{I_1} + H_{ac}^{I_1},\\
H_{al}^{I_1} &= \sum_{k=1,2,3} \Omega_k(t)|e\rangle_k\langle f| + H.c.,\\
H_{ac}^{I_1} &= U H_{ac}^I U^\dagger\\
&= \frac{\lambda_1}{2}|e\rangle_1\langle g|\left[-\sqrt{2}q_1 e^{i\Delta t} + q_2 e^{i(\Delta-\sqrt{2}v)t}\right.\\
&\quad \left. + q_3 e^{i(\Delta+\sqrt{2}v)t}\right] + \frac{\lambda_2}{\sqrt{2}}|e\rangle_2\langle g|\left[q_2 e^{i(\Delta-\sqrt{2}v)t}\right.\\
&\quad \left. - q_3 e^{i(\Delta+\sqrt{2}v)t}\right] + \frac{\lambda_3}{2}|e\rangle_3\langle g|\\
&\quad \times\left[\sqrt{2}q_1 e^{i\Delta t} + q_2 e^{i(\Delta-\sqrt{2}v)t} + q_3 e^{i(\Delta+\sqrt{2}v)t}\right] + H.c.
\end{aligned} \tag{3}$$

We set $\frac{\lambda_1}{\sqrt{2}} = \frac{\lambda_2}{\sqrt{2}} = \frac{\lambda_3}{\sqrt{2}} = \lambda$, $q_2 = a$, and $\Delta = \sqrt{2}v$. Under the large detuning regime $\{\Delta, \Delta + \sqrt{2}v\} \gg \lambda$, the Hamiltonian $H_{ac}^{I_1}$ is simplified as:

$$H_{ac}^{I_1} = \frac{\lambda}{\sqrt{2}}|e\rangle_1\langle g|a + \lambda|e\rangle_2\langle g|a + \frac{\lambda}{\sqrt{2}}|e\rangle_3\langle g|a + H.c. \tag{4}$$

If the initial state is $|\psi_0\rangle = -|g\rangle_1|f\rangle_2|g\rangle_3|0\rangle_c$, the whole system evolves in the subspace spanned by:

$$\begin{aligned}
|\psi_1\rangle &= |g\rangle_1|f\rangle_2|g\rangle_3|0\rangle_c,\\
|\psi_2\rangle &= |g\rangle_1|e\rangle_2|g\rangle_3|0\rangle_c,\\
|\psi_3\rangle &= |g\rangle_1|g\rangle_2|g\rangle_3|1\rangle_c,\\
|\psi_4\rangle &= |e\rangle_1|g\rangle_2|g\rangle_3|0\rangle_c,\\
|\psi_5\rangle &= |f\rangle_1|g\rangle_2|g\rangle_3|0\rangle_c,\\
|\psi_6\rangle &= |g\rangle_1|g\rangle_2|e\rangle_3|0\rangle_c,\\
|\psi_7\rangle &= |g\rangle_1|g\rangle_2|f\rangle_3|0\rangle_c.
\end{aligned} \tag{5}$$

In this case, we set $\Omega_1(t) = \Omega_3(t) = \Omega(t)$ and use two orthogonal vectors $|\varpi\rangle = \frac{1}{\sqrt{2}}(|\psi_4\rangle + |\psi_6\rangle)$ and $|\widetilde{\varpi}\rangle = \frac{1}{\sqrt{2}}(|\psi_4\rangle - |\psi_6\rangle)$ to rewrite the Hamiltonian H_I. We can obtain

$$\begin{aligned}
H_I &= H_{al}^{I_1} + H_{ac}^{I_1},\\
H_{al}^{I_1} &= \Omega_2(t)|\psi_1\rangle\langle\psi_2| + \frac{\Omega(t)}{\sqrt{2}}(|\psi_5\rangle + |\psi_7\rangle)\langle\varpi|\\
&\quad + \frac{\Omega(t)}{\sqrt{2}}(|\psi_5\rangle - |\psi_7\rangle)\langle\widetilde{\varpi}| + H.c.,\\
H_{ac}^{I_1} &= \lambda(|\psi_2\rangle + |\varpi\rangle)\langle\psi_3| + H.c.
\end{aligned} \tag{6}$$

It is obvious that when the initial state is $|\psi_1\rangle$, the terms containing $|\widetilde{\varpi}\rangle$ are negligible because they are decoupled to the time evolution of initial state. After that, the Hamiltonian H_I becomes the following form:

$$\begin{aligned}
H_I' &= H_{al}' + H_{ac}',\\
H_{al}' &= \Omega_2(t)|\psi_1\rangle\langle\psi_2| + \frac{\Omega(t)}{\sqrt{2}}(|\psi_5\rangle + |\psi_7\rangle)\langle\varpi| + H.c.,\\
H_{ac}' &= \lambda(|\psi_2\rangle + |\varpi\rangle)\langle\psi_3| + H.c.
\end{aligned} \tag{7}$$

In addition, there are two eigenstates with zero eigenvalues for the intermediate Hamiltonian $H_{ac}^{I_1}$ in the subspace spanned by $\{|\psi_2\rangle, |\psi_3\rangle, |\psi_4\rangle, |\psi_6\rangle\}$,

$$\begin{aligned}
|\varphi_1\rangle &= \frac{\sqrt{6}}{3}\left(-\frac{\sqrt{2}}{2}|\psi_2\rangle + |\psi_4\rangle\right),\\
|\varphi_2\rangle &= \frac{\sqrt{6}}{3}\left(-\frac{\sqrt{2}}{2}|\psi_2\rangle + |\psi_6\rangle\right).
\end{aligned} \tag{8}$$

After orthogonalizing the states $|\varphi_1\rangle$ and $|\varphi_2\rangle$, we obtain a special dark state $|\phi_1\rangle$ as:

$$|\phi_1\rangle = \frac{1}{\sqrt{2}}(-|\psi_2\rangle + |\varpi\rangle). \tag{9}$$

At the same time, two eigenstates with non-zero eigenvalues for the intermediate Hamiltonian $H_{ac}^{I_1}$ are:

$$\begin{aligned}
|\phi_2\rangle &= \frac{1}{2}(|\psi_2\rangle + \sqrt{2}|\psi_3\rangle + |\varpi\rangle),\\
|\phi_3\rangle &= \frac{1}{2}(|\psi_2\rangle - \sqrt{2}|\psi_3\rangle + |\varpi\rangle),
\end{aligned} \tag{10}$$

with eigenvalues $E_2 = \sqrt{2}\lambda$ and $E_3 = -\sqrt{2}\lambda$. In light of QZD, we rewrite the Hamiltonian H_I' with $|\psi_1\rangle$, $|\phi_1\rangle$, $|\phi_2\rangle$, $|\phi_3\rangle$, and $|\phi_4\rangle = \frac{1}{\sqrt{2}}(|\psi_5\rangle + |\psi_7\rangle)$ ($|\phi_4\rangle$ is the target state.),

$$\begin{aligned}
H_I' &= H_{al}' + H_{ac}',\\
H_{al}' &= \frac{\Omega_2(t)}{\sqrt{2}}(-|\psi_1\rangle\langle\phi_1|) + \frac{\Omega_2(t)}{2}(|\psi_1\rangle\langle\phi_2|)\\
&\quad + \frac{\Omega_2(t)}{2}(|\psi_1\rangle\langle\phi_3|) + \frac{\Omega(t)}{\sqrt{2}}(|\phi_4\rangle\langle\phi_1|)\\
&\quad + \frac{\Omega(t)}{2}(|\phi_4\rangle\langle\phi_2|) + \frac{\Omega(t)}{2}(|\phi_4\rangle\langle\phi_3|) + H.c.,\\
H_{ac}' &= \sqrt{2}\lambda(|\phi_2\rangle\langle\phi_2| - |\phi_3\rangle\langle\phi_3|).
\end{aligned} \tag{11}$$

We introduce two vectors $|\mu_1\rangle = \frac{1}{\sqrt{2}}(|\phi_2\rangle - |\phi_3\rangle)$ and $|\mu_2\rangle = \frac{1}{\sqrt{2}}(|\phi_2\rangle + |\phi_3\rangle)$ for rewriting the Hamiltonian H_I'. The Hamiltonian H_I' becomes the following form:

$$\begin{aligned}
H_{re} &= \frac{|\phi_1\rangle}{\sqrt{2}}(-\Omega_2(t)\langle\psi_1| + \Omega(t)\langle\phi_4|)\\
&\quad + \frac{|\mu_2\rangle}{\sqrt{2}}(\Omega_2(t)\langle\psi_1| + \Omega(t)\langle\phi_4|)\\
&\quad + \sqrt{2}\lambda|\mu_1\rangle\langle\mu_2| + H.c.
\end{aligned} \tag{12}$$

There is a dark state for the Hamiltonian H_{re},

$$|\theta_0\rangle = \frac{1}{N}[\Omega(t)|\psi_1\rangle - \frac{\Omega_2(t)\Omega(t)}{\lambda}|\mu_1\rangle + \Omega_2(t)|\phi_4\rangle], \tag{13}$$

with

$$N = \sqrt{\Omega_2^2(t) + \Omega^2(t) + (\Omega_2(t)\Omega(t)/\lambda)^2}.$$

For the Hamiltonian H_{re}, the status of the system can be expressed by using this $|\widetilde{\psi}(t)\rangle = \sum_{l=0}^{4} B_l(t)|\theta_l(t)\rangle$ at any

time, where $|\theta_l(t)\rangle$ denotes the instantaneous eigenstates of H_{re}. The corresponding eigenvalues of $|\theta_l(t)\rangle$ is ξ_l. We know that the construction of nonadiabatic process is the simplest way of speeding up the evolution for the system. The adiabatic condition $\langle\theta_0(t)|\partial_t\theta_{3(4)}(t)\rangle \ll \xi_{3(4)}$ is fulfilled, so $B_3(t) = B_4(t) \approx 0$ and the eigenstates $|\theta_3(t)\rangle$ and $|\theta_4(t)\rangle$ do not have chance to participate in the evolution, while the eigenstates $|\theta_1(t)\rangle$ and $|\theta_2(t)\rangle$ whose eigenvalues ξ_1 and ξ_2 are closest to zero would have chance to participate in the evolution [44].

$$
\begin{aligned}
|\theta_1(t)\rangle = \frac{1}{N_e}\Bigg\{ & \frac{\Omega_2(t)}{\varsigma}\left[\frac{\vartheta^2}{2} - \left(\Omega^2(t) + 2\lambda^2\right)\right]|\psi_1\rangle \\
& - \frac{\Omega(t)}{\varsigma}\left[\frac{\vartheta^2}{2} - \left(\Omega_2^2(t) + 2\lambda^2\right)\right]|\phi_4\rangle \\
& - \frac{\vartheta\left(2\lambda^2+\eta\right)}{2\varsigma}|\phi_1\rangle - \frac{\vartheta}{2\lambda}|\mu_2\rangle + |\mu_1\rangle\Bigg\}, \\
|\theta_2(t)\rangle = \frac{1}{N_e}\Bigg\{ & \frac{\Omega_2(t)}{\varsigma}\left[\frac{\vartheta^2}{2} - \left(\Omega^2(t) + 2\lambda^2\right)\right]|\psi_1\rangle \\
& - \frac{\Omega(t)}{\varsigma}\left[\frac{\vartheta^2}{2} - \left(\Omega_2^2(t) + 2\lambda^2\right)\right]|\phi_4\rangle \\
& + \frac{\vartheta\left(2\lambda^2+\eta\right)}{2\varsigma}|\phi_1\rangle + \frac{\vartheta}{2\lambda}|\mu_2\rangle + |\mu_1\rangle\Bigg\}, \qquad (14)
\end{aligned}
$$

with

$$
\begin{aligned}
\eta &= \sqrt{(\Omega_2^2(t) - \Omega^2(t))^2 + 4\lambda^4}, \\
\vartheta &= \sqrt{\Omega_2^2(t) + \Omega^2(t) + 2\lambda^2 - \eta}, \\
\varsigma &= \lambda(\Omega_2^2(t) - \Omega^2(t)),
\end{aligned}
$$

and N_e is the corresponding normalization coefficient. Through analysing the proportions of the base vectors in equation (12) in the eigenstates $|\theta_1(t)\rangle$ and $|\theta_2(t)\rangle$, the coefficients ratio τ for states $|\phi_1\rangle$ and $|\mu_2\rangle$ is:

$$
\tau = \left|\left[\frac{\vartheta\left(2\lambda^2+\eta\right)}{2\varsigma}\right] \Big/ \left(\frac{\vartheta}{2\lambda}\right)\right| = \left|\frac{2\lambda^2+\eta}{\Omega_2^2(t) - \Omega^2(t)}\right|, \qquad (15)
$$

when $\tau^2 \gg 1$, the population of the state $|\mu_2\rangle$ is far less than that of the state $|\phi_1\rangle$. So we assume that $\tau^2 \gg 1$ is established in the whole evolution process and the state $|\mu_2\rangle$ is considered as negligible. Then, the whole system can be divided into two parts: the main subsystem $S_m = \{|\psi_1\rangle, |\phi_1\rangle, |\phi_4\rangle\}$ and the assistant subsystem $S_n = \{|\mu_1\rangle\}$. They are independent of each other. The Hamiltonian for the main subsystem is

$$
H_m = \frac{|\phi_1\rangle}{\sqrt{2}}(-\Omega_2(t)\langle\psi_1| + \Omega(t)\langle\phi_4|) + H.c. \qquad (16)
$$

In order to construct the shortcuts for generating two-atom maximally entangled state by the dynamics of invariant-based inverse engineering, we need to find out the Hermitian invariant operator $I(t)$, which satisfies $i\partial_t I(t) = [H_m, I(t)]$. Since H_m possesses SU(2) dynamical symmetry [48], $I(t)$ can be easily given [35]

$$
\begin{aligned}
I(t) = \frac{\sqrt{\Omega_2(t)^2 + \Omega(t)^2}}{\sqrt{2}}(\cos\gamma\sin\beta|\phi_1\rangle\langle\psi_1| \\
+ \cos\gamma\cos\beta|\phi_1\rangle\langle\phi_4| + i\sin\gamma|\phi_4\rangle\langle\psi_1| + H.c.),
\end{aligned} \qquad (17)
$$

γ and β are both time-dependent auxiliary parameters. $\Omega_2(t)$ and $\Omega(t)$ are obtained through solving the relation $i\partial_t I(t) = [H_m, I(t)]$,

$$
\begin{aligned}
\Omega_2(t) &= \sqrt{2}(\dot\beta\cot\gamma\sin\beta + \dot\gamma\cos\beta), \\
\Omega(t) &= \sqrt{2}(\dot\beta\cot\gamma\cos\beta - \dot\gamma\sin\beta),
\end{aligned} \qquad (18)
$$

where the dot represents a time derivative. The general solution of the Schrödinger equation $i\partial_t|\psi\rangle = H_m|\psi\rangle$ with respect to the instantaneous eigenstates of $I(t)$ is written as:

$$
|\psi(t)\rangle = \sum_{n=0,\pm} C_n e^{i\alpha_n}|\widetilde{\theta}_n(t)\rangle, \qquad (19)
$$

where α_n are the LR phases [35,49]

$$
\alpha_n(t_f) = \int_0^{t_f}\langle\widetilde{\theta}_n(t)|\left[i\frac{\partial}{\partial t} - H_m(t)\right]|\widetilde{\theta}_n(t)\rangle dt, \qquad (20)
$$

t_f is the total interaction time. In our case $\alpha_0 = 0$ and

$$
\begin{aligned}
\alpha_\pm = \mp\int_0^{t_f}\Bigg[\dot\beta\sin\gamma + \frac{1}{\sqrt{2}}\Big(\Omega_2(t)\sin\beta \\
+ \Omega(t)\cos\beta\Big)\cos\gamma\Bigg]dt,
\end{aligned} \qquad (21)
$$

$|\widetilde{\theta}_n(t)\rangle$ are the instantaneous eigenstates of $I(t)$,

$$
\begin{aligned}
|\widetilde{\theta_0}(t)\rangle &= \cos\gamma\cos\beta|\psi_1\rangle - i\sin\gamma|\phi_1\rangle - \cos\gamma\sin\beta|\phi_4\rangle, \\
|\widetilde{\theta}_\pm(t)\rangle &= \frac{1}{\sqrt{2}}[(\sin\gamma\cos\beta \pm i\sin\beta)|\psi_1\rangle + i\cos\gamma|\phi_1\rangle \\
&\quad - (\sin\gamma\sin\beta \mp i\cos\beta)|\phi_4\rangle].
\end{aligned} \qquad (22)
$$

In order to transfer the population from the initial state $|\psi_1\rangle$ to the target state $-|\phi_4\rangle$, we choose the parameters appropriately

$$
\gamma(t) = \epsilon, \beta(t) = \pi t/2t_f, \qquad (23)
$$

where ϵ is a time-independent small value and t_f is the interaction time. It should be noted that the parameters $\Omega_2(t)$ and $\Omega(t)$ are closely related to $\gamma(t)$. In a single-eigenstate evolution process (singlemode driving), $\gamma(t)$ generally is a polynomial [36], the pulses' shapes may be difficult to be realized in practice. However, in a multi-eigenstate evolution process (multimode driving), $\gamma(t)$ is chosen as a small constant value [43–45]. After the precise calculation, we can easily obtain

$$
\begin{aligned}
\Omega_2(t) &= \frac{\pi\cot\epsilon}{\sqrt{2}t_f}\sin\frac{\pi t}{2t_f}, \\
\Omega(t) &= \frac{\pi\cot\epsilon}{\sqrt{2}t_f}\cos\frac{\pi t}{2t_f}.
\end{aligned} \qquad (24)
$$

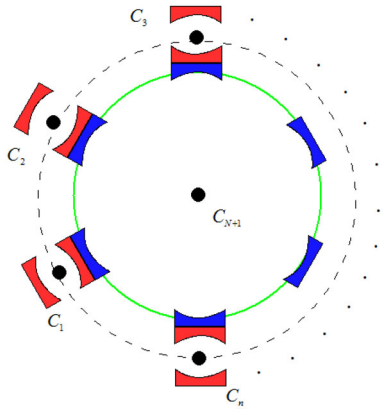

Fig. 2. The cavity-atom combined system for controlled N-atom W state generation. The control qubit in the cavity C_{N+1}, the N controlled qubits in N cavities C_1, C_2, ..., C_N, respectively.

In the present case, when $t = t_f$

$$|\psi(t_f)\rangle = i\sin\epsilon\sin\alpha|\psi_1\rangle + i\sin\epsilon\cos\epsilon(\cos\alpha - 1)|\phi_1\rangle - (\cos^2\epsilon + \sin^2\epsilon\cos\alpha)|\phi_4\rangle, \quad (25)$$

where $\alpha = \pi/(2\sin\epsilon) =| \alpha_\pm |$. Hence, when we choose $\alpha = 2j\pi$ ($j = \pm1, \pm2, \ldots$), $|\psi(t_f)\rangle = -|\phi_4\rangle$ can be obtained. In the assistant subsystem S_n, the time-dependent population of the state $|\mu_2\rangle$ is mainly dominated by the dark state evolution [44]. Its population becomes zero and the dark state also evolves into the state $-|\phi_4\rangle$ when $t = t_f$. With the help of both the subsystems S_m and S_n, the whole system quickly evolves from the initial state $|\psi_1\rangle$ to the final state $-|\phi_4\rangle$ [$|\phi_4\rangle = \frac{1}{\sqrt{2}}(|\psi_5\rangle + |\psi_7\rangle) = \frac{1}{\sqrt{2}}(|f\rangle_1|g\rangle_3 + |g\rangle_1|f\rangle_3)|g\rangle_2|0\rangle_c$]. So, we can see that atom 1 and atom 3 are in the two-atom maximally entangled state.

3 Fast controlled preparation of N-atom W state in N + 1 directly coupled cavities via shortcuts to adiabatic passage

Actually, the above scheme in Section 2 can be effectively applied to $(N+1)$-atom ($N \geq 3$) systems for fast controlled generating N-atom W state. As shown in Figure 2, the $N+1$ atoms are trapped in the $N+1$ cavities, respectively (here, we choose the $(N+1)$th qubit as the control qubit). In the interaction picture, the whole Hamiltonian of cavity-atom combined systems can be described as:

$$\begin{aligned} H_i'' &= H_{al}'' + H_{ac}'' + H_c'', \\ H_{al}'' &= \sum_{k=1,2,3,\ldots,N+1} \Omega_k(t)|e\rangle_k\langle f| + H.c., \\ H_{ac}'' &= \sum_{k=1,2,3,\ldots,N+1} \lambda_k a_k e^{i\Delta t}|e\rangle_k\langle g| + H.c., \\ H_c'' &= \sum_{n=1,2,3,\ldots,N} v a_n^\dagger a_{N+1} + H.c., \end{aligned} \quad (26)$$

where H_{al}'' is the Hamiltonian for the interaction between the atoms and the time-dependent laser pulses, H_{ac}'' is the Hamiltonian for the interaction between the atoms and the cavities, and H_c'' is the Hamiltonian for the direct interaction between the coupled cavities.

We solve the eigenequation of Hamiltonian H_c'', getting the following bosonic operators

$$\begin{aligned} q_m &= \frac{1}{\sqrt{2}}(-a_1 + a_{m+1}), (m = 1, 2, \ldots N-1), \\ q_N &= \frac{1}{\sqrt{2N}}(a_1 + a_2 + \ldots + a_N + \sqrt{N}a_{N+1}), \\ q_{N+1} &= \frac{1}{\sqrt{2N}}(a_1 + a_2 + \ldots + a_N - \sqrt{N}a_{N+1}). \end{aligned} \quad (27)$$

We rewrite the Hamiltonian H_c'' with the bosonic operators and obtain $H_c'' = \sqrt{N}v(q_N^\dagger q_N - q_{N+1}^\dagger q_{N+1})$. In the rotation framework, we perform the unitary transformation $U = e^{iH_c''t}$. After that, we set $\frac{\lambda_1}{\sqrt{2}} = \frac{\lambda_2}{\sqrt{2}} = \ldots = \frac{\lambda_{N+1}}{\sqrt{2}} = \lambda'$, $q_N = a$, and $\Delta = \sqrt{N}v$. Under the large detuning regime $\{\Delta, \Delta + \sqrt{N}v\} \gg \lambda'$ condition, the Hamiltonian H_{ac}'' becomes

$$\begin{aligned} H_{ac'}'' &= e^{iH_c''t}H_{ac}''e^{-iH_c''t} \\ &= \frac{\lambda'}{\sqrt{N}}|e\rangle_1\langle g|a + \frac{\lambda'}{\sqrt{N}}|e\rangle_2\langle g|a + \ldots \\ &\quad + \frac{\lambda'}{\sqrt{N}}|e\rangle_N\langle g|a + \lambda'|e\rangle_{N+1}\langle g|a + H.c. \end{aligned} \quad (28)$$

If the initial state is:

$$|\psi_0'\rangle = -|g\rangle_1|g\rangle_2|g\rangle_3\ldots|g\rangle_N|f\rangle_{N+1}|0\rangle_c,$$

the whole system evolves in the subspace spanned by:

$$\begin{aligned} |\psi_1'\rangle &= |g\rangle_1|g\rangle_2|g\rangle_3\ldots|g\rangle_N|f\rangle_{N+1}|0\rangle_c, \\ |\psi_2'\rangle &= |g\rangle_1|g\rangle_2|g\rangle_3\ldots|g\rangle_N|e\rangle_{N+1}|0\rangle_c, \\ |\psi_3'\rangle &= |g\rangle_1|g\rangle_2|g\rangle_3\ldots|g\rangle_N|g\rangle_{N+1}|1\rangle_c, \\ |\psi_4'\rangle &= |g\rangle_1|g\rangle_2|g\rangle_3\ldots|g\rangle_{N-1}|e\rangle_N|g\rangle_{N+1}|0\rangle_c, \\ |\psi_5'\rangle &= |g\rangle_1|g\rangle_2|g\rangle_3\ldots|g\rangle_{N-1}|f\rangle_N|g\rangle_{N+1}|0\rangle_c, \\ &\vdots \\ |\psi_{2N+2}'\rangle &= |e\rangle_1|g\rangle_2|g\rangle_3\ldots|g\rangle_N|g\rangle_{N+1}|0\rangle_c, \\ |\psi_{2N+3}'\rangle &= |f\rangle_1|g\rangle_2|g\rangle_3\ldots|g\rangle_N|g\rangle_{N+1}|0\rangle_c. \end{aligned} \quad (29)$$

There are N eigenstates with zero eigenvalues for the intermediate Hamiltonian $H_{ac'}''$ in the subspace spanned by $\{|\psi_2'\rangle, |\psi_3'\rangle, |\psi_4'\rangle, |\psi_6'\rangle, \ldots, |\psi_{2N+2}'\rangle\}$. After orthogonalizing the dark states for the Hamiltonian $H_{ac'}''$, we get a special dark state $|\phi_1'\rangle$

$$|\phi_1'\rangle = \frac{1}{\sqrt{2}}\left[-|\psi_2'\rangle + \frac{1}{\sqrt{N}}\left(|\psi_4'\rangle + |\psi_6'\rangle + \ldots + |\psi_{2N+2}'\rangle\right)\right]. \quad (30)$$

For convenience, we assume $|\varpi'\rangle = \frac{1}{\sqrt{N}}(|\psi_4'\rangle + |\psi_6'\rangle + \ldots + |\psi_{2N+2}'\rangle)$. At the same time, the two eigenstates with

non-zero eigenvalues for the Hamiltonian $H''_{ac'}$ are

$$|\phi'_2\rangle = \frac{1}{2}(|\psi'_2\rangle + \sqrt{2}|\psi'_3\rangle + |\varpi'\rangle),$$
$$|\phi'_3\rangle = \frac{1}{2}(|\psi'_2\rangle - \sqrt{2}|\psi'_3\rangle + |\varpi'\rangle), \quad (31)$$

with eigenvalues $E_2 = \sqrt{N}\lambda'$ and $E_3 = -\sqrt{N}\lambda'$. Afterwards, we set $\Omega_1(t) = \Omega_2(t) = \ldots = \Omega_N(t) = \Omega'(t)$, $|\phi'_4\rangle = \frac{1}{\sqrt{N}}(|\psi'_5\rangle + |\psi'_7\rangle + \ldots + |\psi'_{2N+3}\rangle)$ ($|\phi'_4\rangle$ is the target state.), $|\mu'_1\rangle = \frac{1}{\sqrt{2}}(|\phi'_2\rangle - |\phi'_3\rangle)$, and $|\mu'_2\rangle = \frac{1}{\sqrt{2}}(|\phi'_2\rangle + |\phi'_3\rangle)$. According to the analysis in Section 2, we rewrite the Hamiltonian H''_I ($H''_I = H''_{al} + H''_{ac'}$). The Hamiltonian H''_I becomes the following form:

$$H'_{re} = \frac{|\phi'_1\rangle}{\sqrt{2}}(-\Omega_{N+1}(t)\langle\psi'_1| + \Omega'(t)\langle\phi'_4|) + \frac{|\mu'_2\rangle}{\sqrt{2}}(\Omega_{N+1}(t)\langle\psi'_1| + \Omega'(t)\langle\phi'_4|) + \sqrt{N}\lambda'|\mu'_1\rangle\langle\mu'_2| + H.c. \quad (32)$$

There is a dark state for the Hamiltonian H'_{re},

$$|\theta'_0\rangle = \frac{1}{N_1}\left[\Omega'(t)|\psi'_1\rangle - \frac{\sqrt{2}\Omega_{N+1}(t)\Omega'(t)}{\sqrt{N}\lambda'}|\mu'_1\rangle + \Omega_{N+1}(t)|\phi'_4\rangle\right], \quad (33)$$

with

$$N_1 = \sqrt{\Omega^2_{N+1}(t) + \Omega'^2(t) + (\sqrt{2}\Omega_{N+1}(t)\Omega'(t)/\sqrt{N}\lambda')^2}.$$

According to the analysis in Section 2, the coefficients ratio τ' for states $|\phi'_1\rangle$ and $|\mu'_2\rangle$ is

$$\tau' = \left|\frac{N\lambda'^2 + \eta'}{\Omega^2_{N+1}(t) - \Omega'^2(t)}\right|, \quad (34)$$

with $\eta' = \sqrt{(\Omega^2_{N+1}(t) - \Omega'^2(t))^2 + N^2\lambda'^4}$. The Hamiltonian for the main subsystem is

$$H'_m = \frac{|\phi'_1\rangle}{\sqrt{2}}(-\Omega_{N+1}(t)\langle\psi'_1| + \Omega'(t)\langle\phi'_4|) + H.c. \quad (35)$$

In order to construct the shortcuts for generating N-atom W state by the dynamics of invariant-based inverse engineering, we need to find out the Hermitian invariant operator $I(t)$, which satisfies $i\partial_t I(t) = [H'_m, I(t)]$. Since H'_m possesses SU(2) dynamical symmetry [48], $I(t)$ can be easily given [35]

$$I(t) = \frac{\sqrt{\Omega^2_{N+1}(t) + \Omega'^2(t)}}{\sqrt{2}} \times (\cos\gamma\sin\beta|\phi'_1\rangle\langle\psi'_1| + \cos\gamma\cos\beta|\phi'_1\rangle\langle\phi'_4| + i\sin\gamma|\phi'_4\rangle\langle\psi'_1| + H.c.), \quad (36)$$

where γ and β are both time-dependent auxiliary parameters. $\Omega_{N+1}(t)$ and $\Omega'(t)$ are obtained through solving the relation $i\partial_t I(t) = [H'_m, I(t)]$,

$$\Omega_{N+1}(t) = \sqrt{2}(\dot{\beta}\cot\gamma\sin\beta + \dot{\gamma}\cos\beta),$$
$$\Omega'(t) = \sqrt{2}(\dot{\beta}\cot\gamma\cos\beta - \dot{\gamma}\sin\beta), \quad (37)$$

where the dot represents a time derivative. The general solution of the Schrödinger equation $i\partial_t|\psi\rangle = H'_m|\psi\rangle$ with respect to the instantaneous eigenstates of $I(t)$ is written as:

$$|\psi(t)\rangle = \sum_{n=0,\pm} C_n e^{i\alpha_n}|\widetilde{\theta}_n(t)\rangle, \quad (38)$$

where α_n are the LR phases [35,49]

$$\alpha_n(t_f) = \int_0^{t_f}\langle\widetilde{\theta}_n(t)|\left[i\frac{\partial}{\partial t} - H'_m(t)\right]|\widetilde{\theta}_n(t)\rangle dt, \quad (39)$$

t_f is the total interaction time. In our case $\alpha_0 = 0$ and

$$\alpha_\pm = \mp\int_0^{t_f}\left[\dot{\beta}\sin\gamma + \frac{1}{\sqrt{2}}(\Omega_{N+1}(t)\sin\beta + \Omega'(t)\cos\beta)\cos\gamma\right]dt, \quad (40)$$

$|\widetilde{\theta}_n\rangle$ are the instantaneous eigenstates of $I(t)$,

$$|\widetilde{\theta}_0\rangle = \cos\gamma\cos\beta|\psi'_1\rangle - i\sin\gamma|\phi'_1\rangle - \cos\gamma\sin\beta|\phi'_4\rangle,$$
$$|\widetilde{\theta}_\pm\rangle = \frac{1}{\sqrt{2}}[(\sin\gamma\cos\beta \pm i\sin\beta)|\psi'_1\rangle + i\cos\gamma|\phi'_1\rangle - (\sin\gamma\sin\beta \mp i\cos\beta)|\phi'_4\rangle]. \quad (41)$$

In order to transfer the population from the initial state $|\psi'_1\rangle$ to the target state $-|\phi'_4\rangle$, we choose the parameters appropriately

$$\gamma(t) = \epsilon, \beta(t) = \pi t/2t_f, \quad (42)$$

where ϵ is a time-independent small value. From a detailed calculation, we can obtain

$$\Omega_{N+1}(t) = \frac{\pi\cot\epsilon}{\sqrt{2}t_f}\sin\frac{\pi t}{2t_f},$$
$$\Omega'(t) = \frac{\pi\cot\epsilon}{\sqrt{2}t_f}\cos\frac{\pi t}{2t_f}. \quad (43)$$

In the present case, when $t = t_f$

$$|\psi(t_f)\rangle = i\sin\epsilon\sin\alpha|\psi'_1\rangle + i\sin\epsilon\cos\epsilon(\cos\alpha - 1)|\phi'_1\rangle - (\cos^2\epsilon + \sin^2\epsilon\cos\alpha)|\phi'_4\rangle, \quad (44)$$

where $\alpha = \pi/(2\sin\epsilon) = |\alpha_\pm|$. Hence, when we choose $\alpha = 2j\pi$ ($j = \pm1, \pm2, \ldots$), $|\psi(t_f)\rangle = -|\phi'_4\rangle$ can be obtained. The whole system quickly evolves from the initial state $|\psi'_1\rangle$ to the final state $-|\phi'_4\rangle$ [$|\phi'_4\rangle = \frac{1}{\sqrt{N}}(|\psi'_5\rangle + |\psi'_7\rangle + \ldots + |\psi'_{2N+3}\rangle)$]. The N-atom W state is successfully generated.

4 Numerical simulation and discussion

The fidelity of the target state $|\phi_4\rangle$ is given through the relation $F = |\langle\phi_4|\rho(t_f)|\phi_4\rangle|$, where $\rho(t_f)$ is the density operator of the system. We also know that the condition $\tau^2 \gg 1$ is the precondition of the scheme's implementation. Now we discuss how to choose parameters to satisfy the condition $\tau^2 \gg 1$ for generating two-atom maximally entangled state. The fidelity of the target state $|\phi_4\rangle$ versus the values of ϵ and λt_f is depicted in Figure 3a. From Figure 3a, we can see if the evolution time $\lambda t_f > 30$, we can get high-fidelity for any value of ϵ. However, the interaction time is too long. So, we choose $\lambda t_f = 10$ and plot the fidelity of the target state $|\phi_4\rangle$ versus the value of ϵ in Figure 3b. Figure 3b shows the optimal value of ϵ for the highest fidelity of the target state $|\phi_4\rangle$ is about 0.2641 when $\lambda t_f = 10$. The parameters ϵ=0.2641 and $\beta(t_f) = \pi/2$ are chosen for a good fidelity when $t = t_f$, which are brought into equation (24), we can get $\Omega_2(t_f) = \frac{\lambda\pi \cot 0.2641}{10\sqrt{2}}$ and $\Omega(t_f) = 0$. Substituting $\Omega_2(t_f)$ and $\Omega(t_f)$ to equation (15), we obtain $\tau^2 = 37.21$, satisfying the condition $\tau^2 \gg 1$. At the same time, from Figure 3b, we can also obtain two sets of data $\{\epsilon_1 = 0.0959$ and $\tau_1 = 1.0699\}$ and $\{\epsilon_2 = 0.0547$ and $\tau_2 = 1.008\}$ by calculation when $\lambda t_f = 10$ (the subscripts "1" and "2" for the symbol ϵ (τ) denote second-highest wave peak and third-highest wave peak in Fig. 3b, respectively). It is manifest that τ_1 and τ_2 do not satisfy the condition $\tau^2 \gg 1$. As is known to all ϵ should be a time-independent small value. However, based on equation (24), if ϵ is too small, $\Omega_2(t)$ will be too large when t_f is a constant value. So, we make a balance between short interaction time, high fidelity, and the condition $\tau^2 \gg 1$, the parameters are chosen as $\{\epsilon = 0.2641$ and $\lambda t_f = 10\}$. Due to the slightly populated intermediate state $|\mu_2\rangle$, the whole system can not be faultlessly considered as a three-level three-atom system, and the optimal value of ϵ for the whole system will not faultlessly satisfy the condition $\sin\epsilon = \frac{1}{4j}(j = 1, 2, 3, \ldots)$. To confirm that the state $|\mu_2\rangle$ can be neglected in the whole evolution process for our scheme, we also plot the population of the state $|\mu_2\rangle$ in Figure 3c. When $v = 10\lambda/\sqrt{2}$ and $\Delta = \sqrt{2}v$, the detuning is 10 times larger than the coupling constant λ, which meets the validity of the large detuning condition in equation (4).

Now we analyse the efficiency of the STAP for the generation of two-atom maximally entangled state. We know from references [34–36,44,45] that we can shorten the time of the evolution process by increasing the amplitude of the laser pulses. The larger the amplitude, the shorter the interaction time needs. The time dependences of $\Omega_2(t)/\lambda$ and $\Omega(t)/\lambda$ versus λt are shown in Figure 4a. Figure 4b shows that the populations of the initial states $|\psi_1\rangle$ and the target state $|\phi_4\rangle$ versus λt. When $\lambda t = 10$, the population of the state $|\psi_1\rangle$ is close to zero, while the population of the state $|\phi_4\rangle$ is close to 1. In order to show that the scheme is fast, we plot the population of the target state $|\phi_4\rangle$ via STAP and adiabatic passage in Figure 4c, respectively. It can be clearly seen that the population of

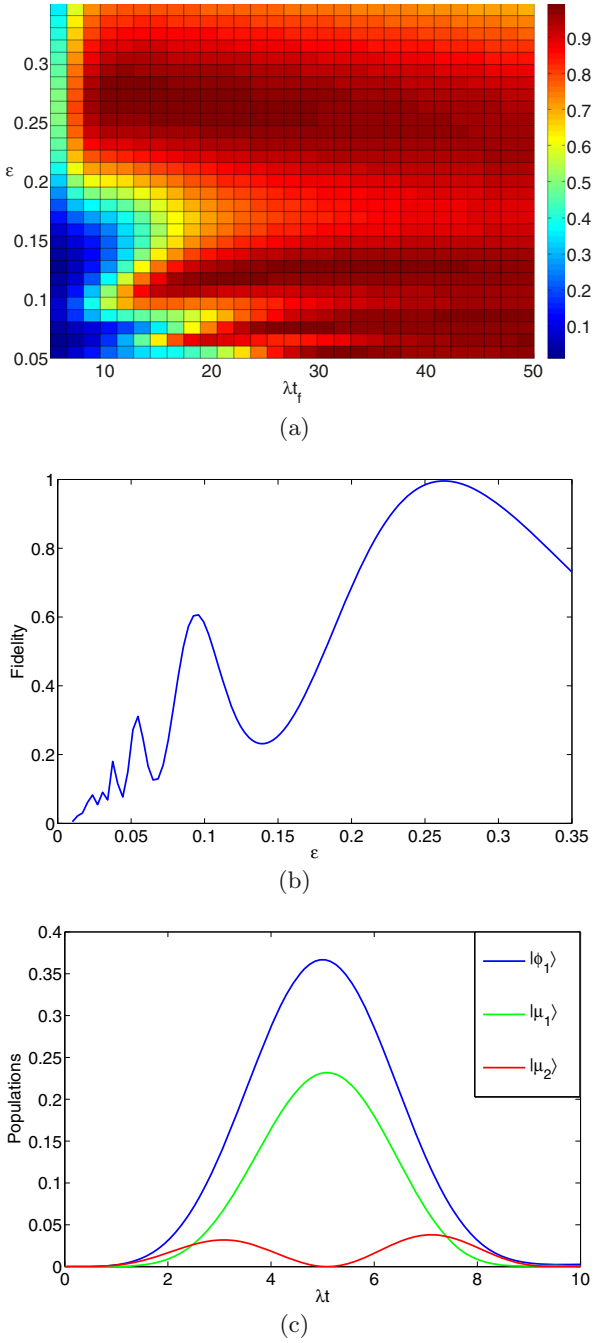

Fig. 3. (a) The fidelity F of the target state $|\phi_4\rangle$ versus the parameter ϵ and the interaction time λt_f. (b) The fidelity F of the target state $|\phi_4\rangle$ versus the parameter ϵ when $\lambda t_f = 10$. (c) Dependence on λt of the populations for the states $|\phi_1\rangle$, $|\mu_1\rangle$, and $|\mu_2\rangle$.

the target state $|\phi_4\rangle$ is 99.56% via STAP when $\lambda t = 10$, however the population of the target state $|\phi_4\rangle$ is 98.65% via adiabatic passage when $\lambda t = 100$ ($\Omega_1(t) = \frac{\lambda}{10}\sin\frac{\pi t}{4t_f}$ and $\Omega_2(t) = \frac{\lambda}{10}\cos\frac{\pi t}{4t_f}$ with the adiabatic method). The result demonstrates that the present STAP is faster than the adiabatic passage.

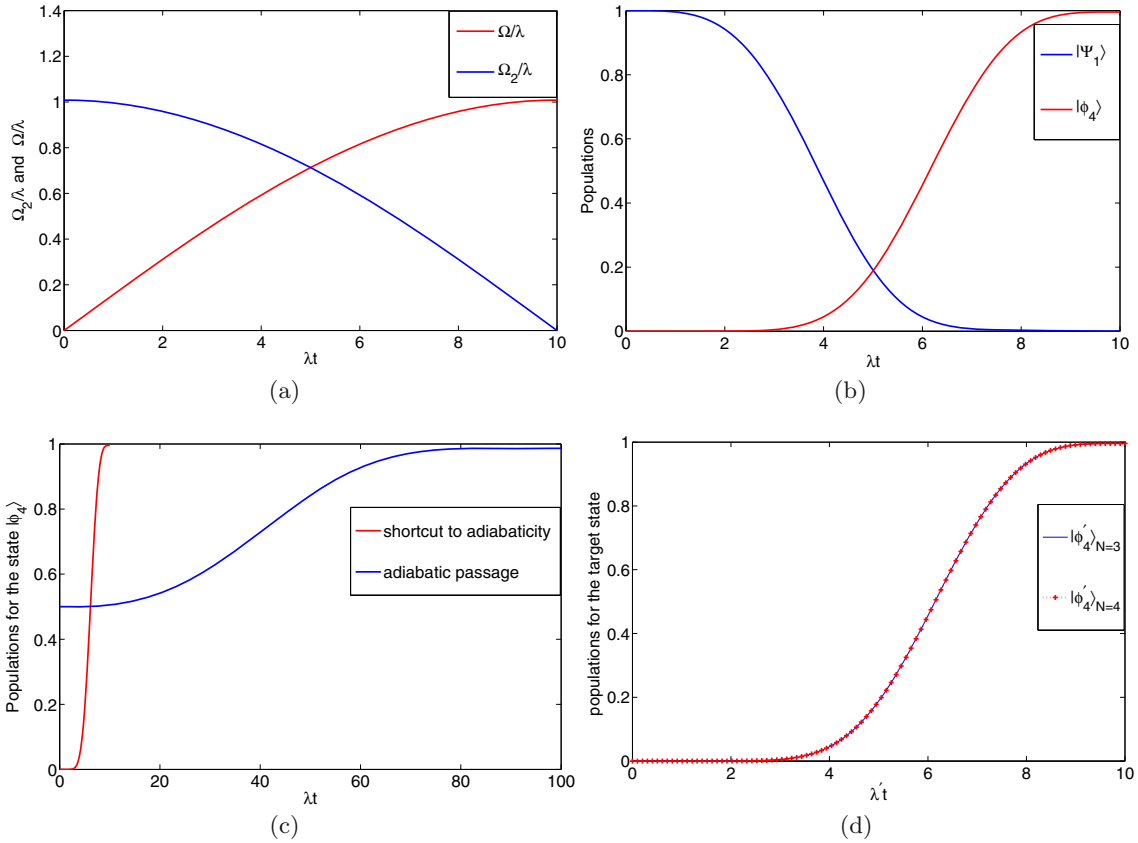

Fig. 4. (a) Dependence on λt of Ω_2/λ and Ω/λ. (b) Dependence on λt of the populations for the initial state $|\psi_1\rangle$ and the target state $|\phi_4\rangle$. (c) The comparison of the operation times required for achieving the target state via the adiabatic method with those via the present STAP method. (d) Dependence on $\lambda' t$ of the populations for three-atom W state $|\phi_4'\rangle_{N=3}$ ($|\phi_4'\rangle_{N=3} = \frac{1}{\sqrt{3}}(|\psi_5'\rangle + |\psi_7' + |\psi_9'\rangle)$) and four-atom W state $|\phi_4'\rangle_{N=4}$ ($|\phi_4'\rangle_{N=4} = \frac{1}{\sqrt{4}}(|\psi_5'\rangle + |\psi_7' + |\psi_9'\rangle + |\psi_{11}'\rangle)$).

We also analyse the efficiency of the STAP for the generation of N-atom W state. As the case stands, the STAP method for the generation of N-atom W state is equivalent to the STAP method for the generation of two-atom maximally entangled state. The parameters $\epsilon = 0.2641$ and $\beta(t_f) = \pi/2$ are chosen for a good fidelity when $t = t_f$, which are brought into equation (43), we can get $\Omega_{N+1}(t_f) = \frac{\lambda' \pi \cot 0.2641}{10\sqrt{2}}$ and $\Omega'(t_f) = 0$. Substituting $\Omega_{N+1}(t_f)$ and $\Omega'(t_f)$ to equation (34), we obtain $\tau'^2 \approx 9N^2$, satisfying the condition $\tau'^2 \gg 1$ when $N \geq 3$. Figure 4d shows the dependence on $\lambda' t$ of the populations for three-atom W state $|\phi_4'\rangle_{N=3}$ ($|\phi_4'\rangle_{N=3} = \frac{1}{\sqrt{3}}(|\psi_5'\rangle + |\psi_7'\rangle + |\psi_9'\rangle)$) and four-atom W state $|\phi_4'\rangle_{N=4}$ ($|\phi_4'\rangle_{N=4} = \frac{1}{\sqrt{4}}(|\psi_5'\rangle + |\psi_7'\rangle + |\psi_9'\rangle + |\psi_{11}'\rangle)$). Figure 4d demonstrates that the interaction time and the fidelity of the N-atom W state are unrelated to the atom number N. The reason is that there are a control qubit and N controlled qubits in the $N+1$ atoms. In the whole evolution process the N controlled atoms are similar to one atom in the cavity. Thus the whole evolution process is equivalent to two atoms in evolution. So, the interaction time and the fidelity of the N-atom W state are unrelated to the atom number N.

When dissipation is considered, the evolution of the system can be modelled by a master equation in Lindblad form,

$$\dot{\rho} = i\,[\rho, H_{tot}] + \sum_k \left[L_k \rho L_k^\dagger - \frac{1}{2}(L_k^\dagger L_k \rho + \rho L_k^\dagger L_k)\right], \tag{45}$$

where the L_k are the so-called Lindblad operators [50]. For the two-atom maximally entangled state's scheme, there are nine Lindblad operators:

$$\begin{aligned}
L_1^k &= \sqrt{\kappa_1} a_1, & L_2^k &= \sqrt{\kappa_2} a_2,\\
L_3^k &= \sqrt{\kappa_3} a_3, & L_4^\Gamma &= \sqrt{\Gamma_1}|f\rangle_1\langle e|,\\
L_5^\Gamma &= \sqrt{\Gamma_2}|f\rangle_2\langle e|, & L_6^\Gamma &= \sqrt{\Gamma_3}|f\rangle_3\langle e|,\\
L_7^\Gamma &= \sqrt{\Gamma_4}|g\rangle_1\langle e|, & L_8^\Gamma &= \sqrt{\Gamma_5}|g\rangle_2\langle e|,\\
L_9^\Gamma &= \sqrt{\Gamma_6}|g\rangle_3\langle e|,
\end{aligned} \tag{46}$$

where $\kappa_m (m = 1, 2, 3)$ are the decays of the cavities and $\Gamma_n (n = 1, 2, 3, 4, 5, 6)$ are the spontaneous emissions of atoms. We assume $\kappa_m = \kappa$ and $\Gamma_n = \Gamma/2$. Figure 5a shows the fidelity of the target state $|\phi_4\rangle$ gradually decreases as the two noise resources increase via STAP when

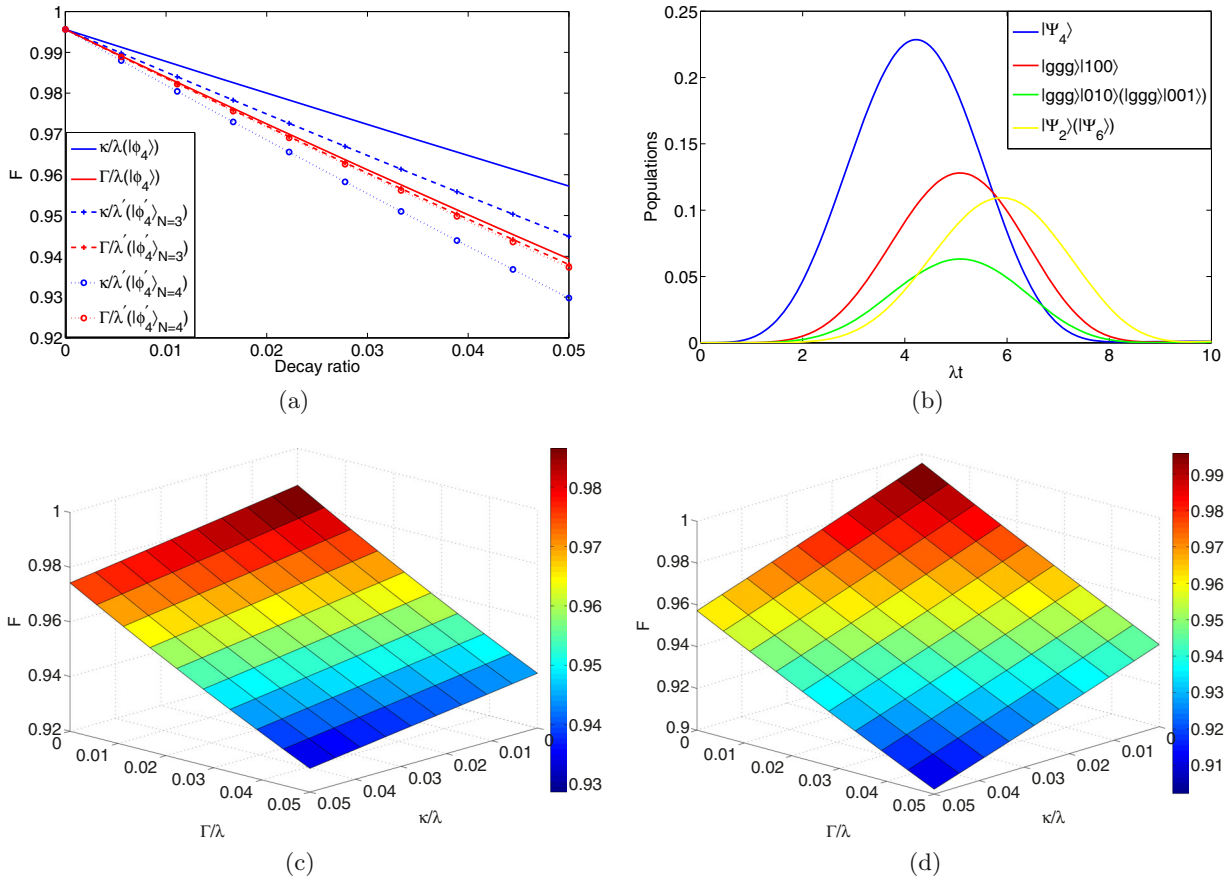

Fig. 5. (a) The influence of decays on the fidelity F of the target state via the STAP method. (b) Dependence on λt of the populations for the intermediate states. (c) The fidelity F of the target state $|\phi_4\rangle$ versus the ratios Γ/λ and κ/λ via the adiabatic method. (d) The fidelity F of the target state $|\phi_4\rangle$ versus the ratios Γ/λ and κ/λ via the STAP method.

$\epsilon = 0.2641$ and $\lambda t_f = 10$. We can find that the decay of spontaneous emission has a greater impact than the decay of cavity on the fidelity. Now we analyze the reasons why the decay of spontaneous emission has a greater impact. In the whole evolution process, the intermediate states also participate the evolution. Among the intermediate states, $|\psi_2\rangle$, $|\psi_4\rangle$, and $|\psi_6\rangle$ can spontaneous radiate to $|g\rangle_1|g\rangle_2|g\rangle_3|000\rangle_c$. Figure 5b shows that the populations of the intermediate states versus λt. The maximum population of the state $|\psi_4\rangle$ reaches 22.85%, so the decay of spontaneous emission has a relatively large impact on the fidelity. The benefits of the STAP method are shown obviously, though the STAP method is sensitive to atomic spontaneous emission, it is robust against cavity decay.

For the N-atom W state, the fidelity of three-atom W state $|\phi_4'\rangle_{N=3}$ and four-atom W state $|\phi_4'\rangle_{N=4}$ versus the two noise resources also are shown in Figure 5a. So, we can expect that when it comes to the generation of N-atom W state, the robustness of the scheme against decoherence caused by the atomic spontaneous emission may remain almost the same as that of the two-atom maximally entangled state. However, the robustness of the scheme against decoherence caused by cavity decay is weaker than that of the two-atom maximally entangled state. It is implied that not only the interaction time for the generation of N-atom W state but also the robustness of the scheme against decoherence caused by the atomic spontaneous emission is insensitive to the atom number N. The reason for this phenomenon is not hard to understand: although the $N+1$ atoms are respectively trapped in the $N+1$ cavities, there are a control qubit and N controlled qubits. In the whole evolution process, the N controlled atoms compose the target state, and the holistic spontaneous emissions of N atoms are similar to one atom in the cavity. The whole evolution process is equivalent to two atoms in evolution. So, the robustness of the scheme against decoherence caused by the atomic spontaneous emission is insensitive to the atom number N. On the other hand, with the increase of the number of coupled cavities, the robustness of the scheme against decoherence caused by cavity decay is weaker, because the decay of N cavities is not equivalent to that of one cavity.

The fidelity of the target state $|\phi_4\rangle$ versus the ratios κ/λ and Γ/λ in the adiabatic method is shown in Figure 5c. The fidelity gradually decreases with the increasing of cavity decay and atomic spontaneous emission. When $\kappa/\lambda = \Gamma/\lambda = 0.05$, the fidelity is 92.87%. The fidelity of the target state $|\phi_4\rangle$ versus the ratios κ/λ and Γ/λ

in the STAP method is shown in Figure 5d. The fidelity gradually decreases with the increasing of cavity decay and atomic spontaneous emission. When $\kappa/\lambda = \Gamma/\lambda = 0.05$, the fidelity is 90.23%. The fidelity of the STAP method is close to the fidelity of the adiabatic method. Therefore, our scheme is robust against the two noise sources and could achieve a better result in realistic conditions. In addition, compared with TQD, the inverse engineering based LR invariant does not have to break down the form of the original Hamiltonian so that the possibility of a nonexistent Hamiltonian which drives the instantaneous eigenstates of the original Hamiltonian exactly in experiment is avoided. The inverse engineering based LR invariant also is more easy and convenient than the fast-forward of quantum dynamics in the laboratory.

The robustness against operational imperfection is also a main factor for the feasibility of the scheme [51]. We calculate the fidelity of the target state $|\phi_4\rangle$ by varying error parameters of the mismatch among the laser amplitude, the interaction time, and coupling constants. We define $\delta x = x' - x$ as the deviation of parameter x. The fidelity of the target state $|\phi_4\rangle$ versus the variations in different parameters are shown in Figures 6a and 6b. As shown in the figures, the scheme is robust against the variations of λ, Ω_0, and T ($\Omega_0 = \frac{\pi \cot 0.2641}{\sqrt{2}t_f}$ and $T = t_f$ is the manipulation time). Figure 6a demonstrates that the scheme is sensitive to the variation of coupling constant υ. This is because the coupling constant υ is strongly related to detuning Δ whose deviation greatly influences the target state's fidelity. However, this is not a serious problem to realize the scheme because the detuning Δ can be precisely controlled in experiment.

In a real experiment, the atom cesium can be used to implement the scheme. The state $|e\rangle$ corresponds to $F = 4, m = 3$ hyperfine state of the $6^2P_{1/2}$ electronic excited state, the state $|g\rangle$ corresponds to $F = 3, m = 2$ hyperfine state of the $6^2S_{1/2}$ electronic ground state, and the state $|f\rangle$ corresponds to $F = 3, m = 4$ hyperfine state of the $6^2S_{1/2}$ electronic ground state, respectively. In recent experimental conditions [52,53], it is predicted to achieve the parameters $\lambda = 2\pi \times 750$ MHz, $\kappa = 2\pi \times 3.5$ MHz, and $\Gamma = 2\pi \times 2.62$ MHz and the optical cavity mode wavelength in a range between 630 and 850 nm. Under the above parameters, we obtain the fidelity of the two-atom maximally entangled state $|\phi_4\rangle$ is about 98.7%, the fidelity of the three-atom W state $|\phi_4'\rangle_{N=3}$ is about 98.6%, and the fidelity of the four-atom W state $|\phi_4'\rangle_{N=4}$ is about 98.4%, which shows our scheme is relatively robust against the realistic conditions. We also know from references [54–57] that the temporal profile of the Rabi frequencies can be well controlled and regulated in recent experiments. Therefore, our scheme may be very promising within current experiment technology.

5 Conclusion

In summary, we have proposed the STAP method for generating two-atom maximally entangled state and N-atom W state in the directly coupled cavities systems.

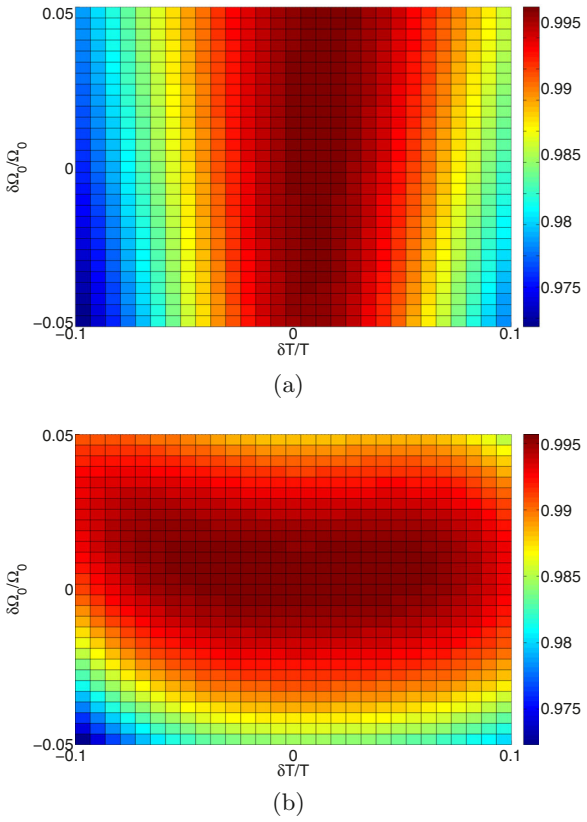

Fig. 6. (a) The fidelity F of the target state $|\phi_4\rangle$ versus the variations of λ and υ. (b) The fidelity F of the target state $|\phi_4\rangle$ versus the variations of Ω_0 and T.

The merits of the method are that we do not need to control the interaction time exactly and the evolution process is fast. When considering dissipation, we find that the method is robust against the decoherences caused by the atomic spontaneous emission and cavity decay. The scheme has a high fidelity and may be implemented with the current experimental technology. So, the scheme is fast, robust, and effective. In addition, the present scheme proves to be useful for applications in scalable distributed quantum networks.

This work was supported by the National Natural Science Foundation of China under Grants Nos. 11575045 and 11374054, the Major State Basic Research Development Program of China under Grant No. 2012CB921601, and the Foundation of Ministry of Education of China under Grant No. 212085.

References

1. H.J. Kimble, Nature **453**, 1023 (2008)
2. S.B. Zheng, G.C. Guo, Phys. Rev. Lett. **85**, 2392 (2000)
3. C.H. Bennett, G. Brassard, C. Crépeau, R. Jozsa, A. Peres, W. Wootters, Phys. Rev. Lett. **70**, 1895 (1993)
4. C.H. Bennett, S.J. Wiesner, Phys. Rev. Lett. **69**, 2881 (1992)
5. A.K. Ekert, Phys. Rev. Lett. **67**, 661 (1991)

6. D. Gottesmanand, I. Chuang, Nature **402**, 390 (1999)
7. J.S. Bell, Physics **1**, 195 (1965)
8. Y. Xia, J. Song, H.S. Song, Appl. Phys. Lett. **92**, 021127 (2008)
9. S.B. Zheng, Eur. Phys. J. D **54**, 719 (2009)
10. W. Dür, G. Vidal, J.I. Cirac, Phys. Rev. A **62**, 062314 (2000)
11. S.B. Zheng, J. Phys. B **7**, 139 (2005)
12. Q.A. Turchette, C.S. Wood, B.E. King, C.J. Myatt, D. Leibfried, W.M. Itano, C. Moroe, D.J. Wineland, Phys. Rev. Lett. **81**, 3631 (1998)
13. E. Hagley, X. Maitre, G. Nogues, C. Wunderlich, M. Brune, J.M. Raimond, S. Haroche, Phys. Rev. Lett. **79**, 1 (1997)
14. A. Rauschenbeutel, G. Nogues, S. Osnaghi, P. Bertet, M. Brune, J.M. Raimond, S. Haroche, Science **288**, 2024 (2000)
15. A. Serafini, S. Mancini, S. Bose, Phys. Rev. Lett. **96**, 010503 (2006)
16. C.D. Ogden, E.K. Irish, M.S. Kim, Phys. Rev. A **78**, 063805 (2008)
17. C. Guerlin, E. Brion, T. Esslinger, K. Mølmer, Phys. Rev. A **82**, 053832 (2010)
18. Z.R. Zhong, X. Lin, B. Zhang, Z.B. Yang, Phys. Scr. **86**, 055008 (2012)
19. E. Collin, G. Ithier, A. Aassime, P. Joyez, D. Vion, D. Esteve, Phys. Rev. Lett. **93**, 157005 (2004)
20. B.T. Torosov, D. Gurin, N.V. Vitanov, Phys. Rev. Lett. **106**, 233001 (2011)
21. L. Allen, J.H. Eberly, *Optical Resonance and Two-Level Atoms* (Dover, New York, 1987), p. 102
22. K. Bergmann, H. Theuer, B.W. Shore, Rev. Mod. Phys. **70**, 1003 (1998)
23. N.V. Vitanov, T. Halfmann, B.W. Shore, K. Bergmann, Annu. Rev. Phys. Chem. **52**, 763 (2001)
24. P. Král, I. Thanopulos, M. Shapiro, Rev. Mod. Phys. **79**, 53 (2007)
25. J.R. Kuklinski, U. Gaubatz, F.T. Hioe, K. Bergmann, Phys. Rev. A **40**, 6741 (1989)
26. S. Masuda, K. Nakamura, Phys. Rev. A **78**, 062108 (2008)
27. S. Masuda, K. Nakamura, Proc. R. Soc. A **466**, 1135 (2010)
28. S. Masuda, K. Nakamura, Phys. Rev. A **84**, 043434 (2011)
29. E. Torrontegui, S. Ibáñez, X. Chen, A. Ruschhaupt, D. Guéry-Odelin, J.G. Muga, Phys. Rev. A **83**, 013415 (2011)
30. E. Torrontegui, S. Martínez-Garaot, A. Ruschhaupt, J.G. Muga, Phys. Rev. A **86**, 013601 (2012)
31. S. Masuda, S.A. Rice, Phys. Rev. A **89**, 033621 (2014)
32. S. Masuda, S.A. Rice, J. Phys. Chem. A **119**, 3479 (2015)
33. M.V. Berry, J. Phys. A **42**, 365303 (2009)
34. X. Chen, I. Lizuain, A. Ruschhaupt, D. Guéry-Odelin, J.G. Muga, Phys. Rev. Lett. **105**, 123003 (2010)
35. X. Chen, E. Torrontegui, J.G. Muga, Phys. Rev. A **83**, 062116 (2011)
36. X. Chen, J.G. Muga, Phys. Rev. A **86**, 033405 (2012)
37. M. Palmero, E. Torrontegui, D. Guéry-Odelin, J.G. Muga, Phys. Rev. A **88**, 053423 (2013)
38. E. Torrontegui, S. Martínez-Garaot, M. Modugno, X. Chen, J.G. Muga, Phys. Rev. A **87**, 033630 (2013)
39. A. Yuste, B. Juliá-Díaz, E. Torrontegui, J. Martorell, J.G. Muga, A. Polls, Phys. Rev. A **88**, 043647 (2013)
40. S. Ibáñez, S. Martínez-Garaot, X. Chen, E. Torrontegui, J.G. Muga, Phys. Rev. A **84**, 023415 (2011)
41. S. Ibáñez, X. Chen, E. Torrontegui, J.G. Muga, A. Ruschhaupt, Phys. Rev. Lett. **109**, 100403 (2012)
42. M. Lu, Y. Xia, L.T. Shen, J. Song, N.B. An, Phys. Rev. A **89**, 012326 (2014)
43. M. Lu, Y. Xia, L.T. Shen, J. Song, Laser Phys. **24**, 105201 (2014)
44. Y.H. Chen, Y. Xia, Q.Q. Chen, J. Song, Phys. Rev. A **89**, 033856 (2014)
45. Y.H. Chen, Y. Xia, Q.Q. Chen, J. Song, Laser Phys. Lett. **11**, 115201 (2014)
46. P. Facchi, S. Pascazio, Phys. Rev. Lett. **89**, 080401 (2002)
47. P. Facchi, G. Marmo, S. Pascazio, J. Phys.: Conf. Ser. **196**, 012017 (2009)
48. Y.Z. Lai, J.Q. Liang, H.J.W. Müller-Kirsten, J.G. Zhou, Phys. Rev. A **53**, 3691 (1996)
49. H.R. Lewis, W.B. Riesenfeld, J. Math. Phys. **10**, 1458 (1969)
50. M.J. Kastoryano, F. Reiter, A.S. Sørensen, Phys. Rev. Lett. **106**, 090502 (2011)
51. Y.H. Chen, Y. Xia, Q.Q. Chen, J. Song, Phys. Rev. A **91**, 012325 (2015)
52. J.R. Buck, H.J. Kimble, Phys. Rev. A **67**, 033806 (2003)
53. S.M. Spillane, T.J. Kippenberg, K.J. Vahala, K.W. Goh, E. Wilcut, H.J. Kimble, Phys. Rev. A **71**, 013817 (2005)
54. D. Kielpinski, J.F. Corney, H.M. Wiseman, Phys. Rev. Lett. **106**, 130501 (2011)
55. C. Hernández-García, J.A. Pérez-Hernández, T. Popmintchev, M.M. Murnane, H.C. Kapteyn, A. Jaron-Becker, A. Becker, L. Plaja, Phys. Rev. Lett. **111**, 033002 (2013)
56. X. Wang, C. Jin, C.D. Lin, Phys. Rev. A **90**, 023416 (2014)
57. N. Berti, W. Ettoumi, S. Hermelin, J. Kasparian, J.P. Wolf, Phys. Rev. A **91**, 063833 (2015)